J Supercond Nov Magn (2014) 27:1991–1995
DOI 10.1007/s10948-014-2554-8

ORIGINAL PAPER

Vortex States and Magnetization Properties in Mesoscopic Superconducting Ring Structures: A Finite-Element Analysis

Lin Peng · Zejiang Wei · Danhua Xu

Received: 8 March 2014 / Accepted: 4 April 2014 / Published online: 7 June 2014

Abstract The time-dependent Ginzburg–Landau equations have been solved numerically by a finite-element analysis for mesoscopic superconducting ring structures with different inner radii. For given applied magnetic fields, we have studied the influences of the inner radius on the vortex states and the magnetization properties of these systems. Our results show that the multivortex states can be stabilized in the mesoscopic superconducting ring with proper inner radius. Magnetization curves show that the magnetic vortices penetrate easily into the superconductor, and the system is magnetized easily for the superconducting ring with smaller inner radius.

Keywords Ginzburg–Landau equations · Mesoscopic superconducting ring · Vortex

1 Introduction

Modern microfabrication and measurement techniques enable one to study the properties of superconducting samples with sizes comparable to the magnetic field penetration depth λ or the coherence length ξ. The behavior of these mesoscopic systems in an external magnetic field is considerably influenced by the boundary conditions besides its size and geometry and may lead to new superconducting states. The mesoscopic samples of different shapes surrounded by vacuum or an insulator medium have been considered extensively both experimentally and theoretically [1–10]. It has been shown that two kinds of superconducting states can exist in these samples, i.e., the giant vortex state [11, 12] and the multivortex state [13–16]. In a superconducting system with circular holes, the superconducting state is characterized by a definite angular momentum that is similar to the Little–Parks oscillations [17]. In 2000, an even more exotic vortex state was predicted to exist in mesoscopic samples with a discrete symmetry (e.g., triangles, squares, regular polygons): the vortex–antivortex state [18], where vortices and antivortices coexist and form the thermodynamically stable ground state. On the other hand, the geometry of a mesoscopic sample can strongly influence the critical field and the current. Especially, by nanostructuring, i.e., the introduction of nanoscale structures (such as holes, pinning centers, and so on) in a superconductor, mesoscopic superconductors can be tuned to exhibit uniquely mesoscopic effects, such as vortices and antivortex configurations [3], vortices trapped in blind holes [19], and so on. These effects are expected to shed light on the d-wave symmetry [20] and the strip structure [21] in high-temperature superconductors.

Recently, an experimental investigation was made of flux jumps and irreversible magnetization of mesoscopic Al superconducting rings, which indicated that the change of vorticity with magnetic field could be larger than unity [7]. A direct observation of vortex states in small superconducting disks for vorticity $L = 0$ to 40 was also reported [22]. Therefore, there still exists a need for alternative proposals of a different system in which the vortex states can be stabilized. The purpose of this paper is to use the finite-element method [4, 16] to determine the magnetic vortex properties of the mesoscopic superconductor rings by solving

L. Peng (✉) · Z. Wei · Danhua Xu
Department of Physics and College of Environmental and Chemical Engineering, Shanghai University of Electric Power, 201300 Shanghai, China
e-mail: plpeng@shiep.edu.cn

L. Peng
Department of Materials, Fudan University, 200433 Shanghai, China

the time-dependent Ginzburg–Landau (TDGL) model. The finite-element method is characterized by approximate solutions that are piecewise polynomial functions with respect to some grid. A specific finite scheme is defined by choosing a particular space of such functions in which to seek approximate solutions. In the present paper, we focus on the influences of the inner radius on the vortex states and the magnetization properties of these systems.

2 Time-Dependent Ginzburg–Landau Model

We consider that the two-dimensional mesoscopic superconducting ring and the external magnetic field $\mathbf{H}$ are uniform and directed normal to the ring plane. For a type II superconductor, the TDGL equations coupled to a penetrating magnetic field $\mathbf{B} = \nabla \times \mathbf{A}$, with $\mathbf{A}$ being the magnetic vector potential, gives an accurate description of the superconducting state of low-T_c superconductors and is well suited to incorporate boundary effects in the treatment of the mesoscopic superconductors. After the normalization and the gauge transformation, the TDGL equations were given by [16, 23]

$$\frac{\partial \psi}{\partial t} = -\left(\frac{i}{\kappa}\nabla + \mathbf{A}\right)^2 \psi + \psi - |\psi|^2 \psi \tag{1}$$

and

$$\sigma \frac{\partial \mathbf{A}}{\partial t} = \frac{i}{2\kappa}\left(\psi \nabla \psi^* - \psi^* \nabla \psi\right) - |\psi|^2 \mathbf{A} - \nabla \times \nabla \times \mathbf{A}, \tag{2}$$

where $\kappa \left(= \lambda / \xi\right)$ is the so-called GL parameter and describes the ability of the sample to screen the applied magnetic field. The λ and ξ denote the London penetration depth and the GL coherence length, respectively. Here, all distances are measured in units of the coherence length $\xi(T) = \xi_0 / \sqrt{1 - T/T_c}$. Temperature T is scaled to T_c. The vector potential $\mathbf{A}$ is expressed in units of $H_{c2}(0)\,\xi(0)$, where the upper critical field is given by $H_{c2}(T) = H_{c2}(0)\left(1 - T/T_c\right)$. The superconducting order parameter ψ in units of $\psi_0 = \sqrt{-\alpha/\beta}$, such that $|\psi|^2 = 1$ in the pure Meissner phase and $|\psi|^2 = 0$ in the normal conducting state (with α and β being the GL coefficients [16]). $|\psi|^2$ represents the local Cooper-pair density. $\mathbf{B} = \nabla \times \mathbf{A}$ stands for the magnetic induction field inside the superconductor.

The vortex state of a small mesoscopic superconductor is strongly influenced by the imposed topological confinement. The shape of the sample boundaries is introduced in our calculation through the Neumann boundary condition, which sets the supercurrent perpendicular to the boundary equal to zero:

$$\mathbf{n} \cdot (-i\nabla - \mathbf{A})\,\psi\,|_{r=R_o} = 0, \tag{3}$$

$$\mathbf{n} \cdot (-i\nabla - \mathbf{A})\,\psi\,|_{r=R_i} = 0, \tag{4}$$

where $\mathbf{n}$ is the normal unit vector on the surface. Suppose the surface of the type II superconductor $\left(\kappa > 1/\sqrt{2}\right)$ in the x-y-plane and a uniform external magnetic field ($\mathbf{H} = (0, 0, H)$) along the z-direction. Thus, the problem is two-dimensional, and the z-component of the magnetic potential is always zero, that is, $\mathbf{A} = (A_x, A_y, 0)$. The initial conditions are $|\psi|^2 = 1$ corresponding to the Meissner state and zero magnetic field inside the superconductor. The calculation is repeated until the relative difference of the order parameter between the two consecutive iteration steps is less than 10^{-6}.

3 Results and Discussions

For circular configurations such as disks, the giant vortex state (or the multivortex state) is characterized by the total angular momentum L [1]. L isthe winding number and gives the vorticity of the system. Due to the nonlinearity of the GL equations, an arbitrary superconducting state is generally a mixture of different angular harmonics L even in axially symmetric systems. Nevertheless, we can introduce an analog to the total angular momentum L, which is still a good quantum number. In sufficiently large disks, the transitions between multivortex states are described by the saddle-point states which correspond to the energy barrier states between those states [24]. Figure 1(a–d) shows the Cooper-pair density $|\psi|^2$ plots in the superconducting rings for the $R_o = 5\xi$ and $R_i = \xi$ at $H/H_{c2} = 0.8$, the $R_o = 5\xi$ and $R_i = 2\xi$ at $H/H_{c2} = 0.8$, the $R_o = 5\xi$ and $R_i = 4$ at $H/H_{c2} = 0.8$, and the $R_o = 5\xi$ and $R_i = 2\xi$ at $H/H_{c2} = 0.8$, respectively. It is observed that strong finite-size effects in conjunction with strong shape effects determine the vortex configuration [1]. When external magnetic field is applied, more flux is easily trapped in the hole for the superconducting ring with smaller inner radius, and eventually the stable multivortex states can be formed inside the superconducting ring. For instance, we can find the multivortex state with $L = 10$ for the case of $R_i = \xi$ and the multivortex state with $L = 7$ for the case of $R_i = 2\xi$ at $H/H_{c2} = 0.8$ (see Fig. 1(a, b)). Meanwhile, at $H/H_{c2} = 1.2$, we observe these multivortex states with $L = 38$, 24, and 12 for the case of $R_i = \xi$, 2ξ, and 3ξ (see Fig. 2 (a–c)), respectively. With increasing inner radius, however, the multivortex states vanish due to strong finite-size effect (see Figs. 1(c, d) and 2(d)), which indicate that the magnetic vortices penetrate easily into the superconducting ring with smaller inner radius. Figure 1(e–h) shows the corresponding vector plots of the supercurrent in the superconducting rings. When a superconducting ring sample is placed in an external magnetic

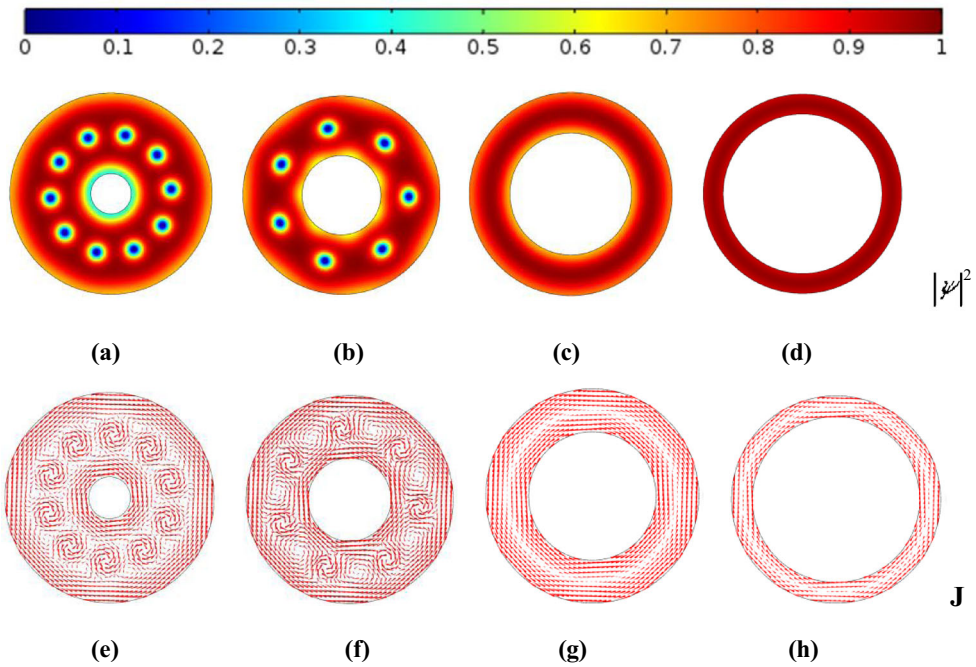

Fig. 1 (Color online) Cooper-pair density $|\psi|^2$ for the rings with $R_i = \xi, 2\xi, 3\xi$, and 4ξ (a, b, c, and d, respectively). Supercurrent **J** for the rings with $R_i = \xi, 2\xi, 3\xi$, and 4ξ (e, f, g, and h, respectively). The other parameter values are $R_o = 5\xi$, $\kappa = 4$, and $H/H_{c2} = 0.8$

field, the magnetic field is expelled from the superconductor due to screening currents near the sample outer boundary. It is clear that the screening currents near the sample outer boundary flow clockwise and the currents near the sample inner boundary counterclockwise, i.e., the magnetic field penetrating the superconductor from the sample inner boundary creates currents flowing in a direction opposite to the screening currents. The competition between these currents and the screening currents results in the existence of vortices [1]. In addition, the vortices also experience inward forces [25]. During the whole process, the vortex–vortex interaction is always repulsive (attractive) between vortices of same (different) sign. Eventually, the vortices will find an equilibrium position, in which the inward and outward forces cancel exactly and the vortices become stable. The similar cases can be found in Fig. 2(e–h).

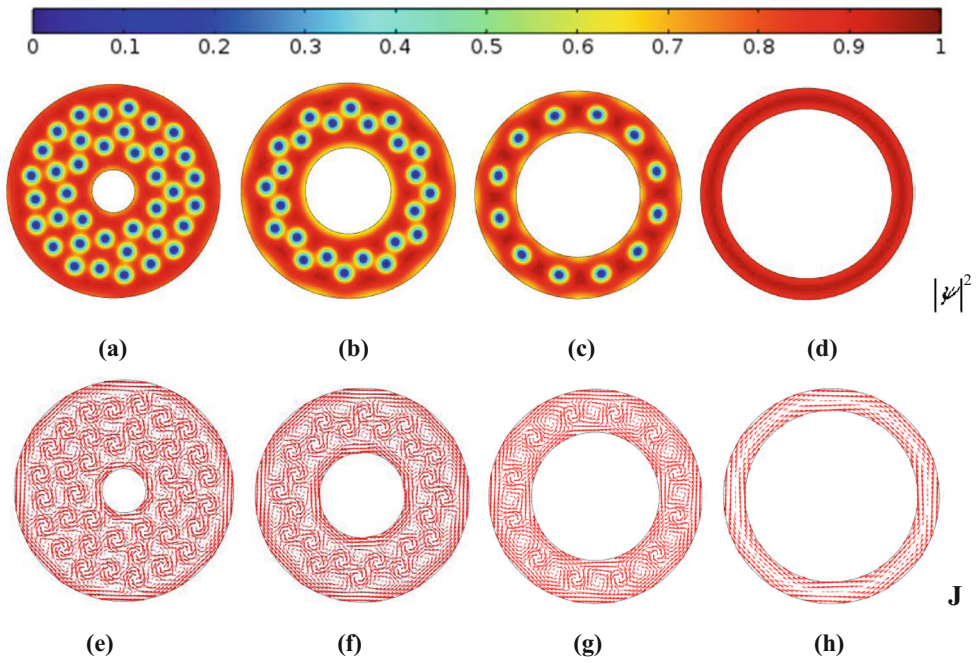

Fig. 2 (Color online) Cooper-pair density $|\psi|^2$ for the rings with $R_i = \xi, 2\xi, 3\xi$, and 4ξ (a, b, c, and d, respectively). Supercurrent **J** for the rings with $R_i = \xi, 2\xi, 3\xi$, and 4ξ (e, f, g, and h, respectively). The other parameter values are $R_o = 5\xi$, $\kappa = 4$, and $H/H_{c2} = 1.2$

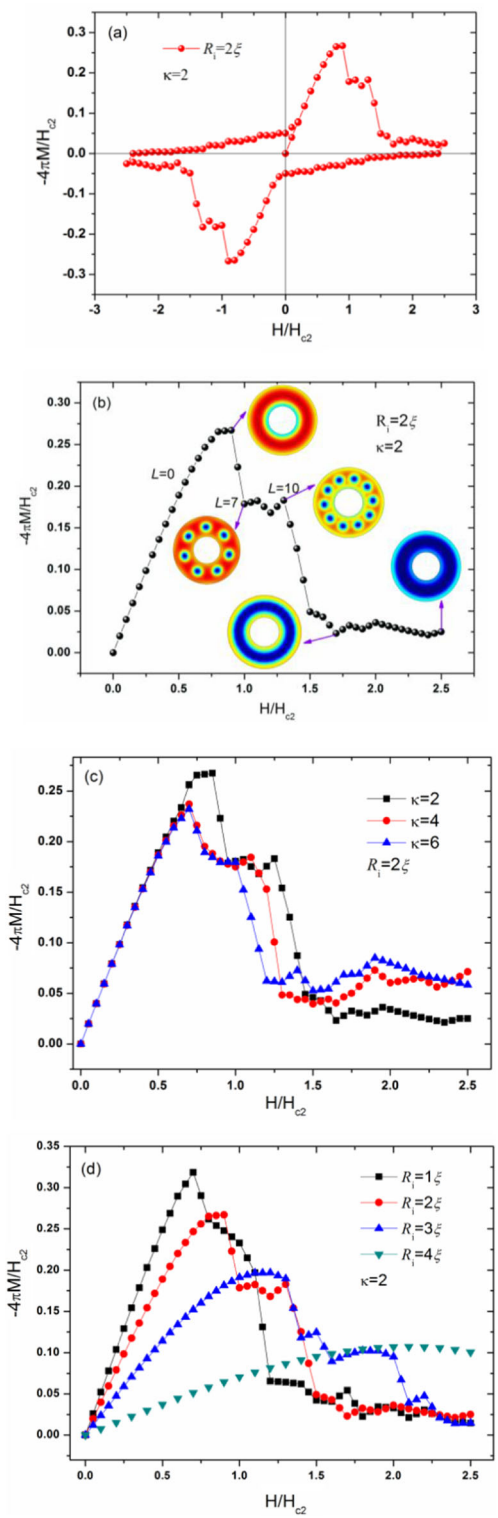

Fig. 3 (Color online) **a** Hysteresis curve of the magnetization M vs the applied magnetic field for $R_o = 5\xi$, $R_i = 2\xi$, and $\kappa = 2$. **b** Magnetization of as a function of applied magnetic field for $R_o = 5\xi$, $R_i = 2\xi$, and $\kappa = 2$. **c** Magnetization of as a function of applied magnetic field for $R_o = 5\xi$, $R_i = 2\xi$, and $\kappa = 2, 4, 6$. **d** Magnetization of as a function of applied magnetic field for $\kappa = 2$, $R_o = 5\xi$, and $R_i = \xi$, 2ξ, 3ξ, and 4ξ. The *insets* show the possible vortex configurations at the relevant magnetic field

Subsequently, the magnetization curves are calculated for the superconducting rings. The external magnetic field is increased from $H/H_{c2} = 0$ to $H/H_{c2} = 2.5$ with the step $\Delta H/H_{c2} = 0.05$. In Fig. 3, the magnetization M vs the external magnetic field are plotted. The area of magnetization $M = \langle B\rangle - H$ can be observed experimentally, which is the difference between the applied field H and the measured field $\langle B\rangle$ [7]. Previously, the individual superconducting and ferromagnetic disks were studied, and an excellent agreement with the above formula was found [2, 5]. Therefore, the dimensionless magnetization in our work, which is a direct measure of the expelled magnetic field from the mesoscopic superconducting ring, can be defined as $M = (\langle B\rangle - H)/4\pi$, where $\langle B\rangle$ is the magnetic induction averaged over the mesoscopic superconducting ring surface area S, i.e., $\langle B\rangle = (1/S)\int B\left(\vec{r}\right)d\vec{r}$. In the initial magnetization process, the superconductor is in the Meissner state. Figure 3a shows the hysteresis curve of the magnetization M vs the external magnetic field for the superconducting ring with the outer radius $R_o = 5\xi$ and inner radius $R_i = 2\xi$. As the magnetic field is applied, the magnetic flux penetrates into the region of order λ near the surface boundary. As the magnetic field is further increased, the magnetization curve shows a peak at $H_p = 0.9$. The system is in the mixed states for $H/H_{c2} > H_p$, which can be proved by the corresponding vortex states (see the insets of Fig. 3b). When the magnetic field is reversed and decreased to $H/H_{c2} < -H_p$, the magnetic flux near the surface boundary is transformed into vortices. Then, they penetrate into the system.

Moreover, the transition field H_p will be decrease with the increasing GL parameter κ (see Fig. 3c). In Fig. 3d, we demonstrate the influence of the inner radius of the superconducting ring on the magnetization behavior. It is observed that the magnetization drops for $H/H_{c2} > H_p$ when the system is in the mixed state and the transition field H_p is strongly influenced by R_i. The smaller the inner radius of the superconducting ring, the smaller the transition field H_p, i.e., the magnetic vortices penetrate easily into the superconductor and the system is magnetized easily.

4 Conclusions

In summary, the time-dependent Ginzburg–Landau equations have been solved numerically by a finite-element analysis for the mesoscopic superconducting ring structures with the different inner radii. We demonstrate that the multivortex states can be stabilized in the mesoscopic superconducting ring with proper inner radius. Magnetization curves show that the magnetic vortices penetrate easily into the superconductor, and the system is magnetized easily for the superconducting ring with the smaller inner radius.

Acknowledgments This work is sponsored by the Natural Science Foundation of Shanghai (No. 13ZR1417600), the Innovation Program of Shanghai Municipal Education Commission (No. 14YZ132), and the Shanghai Science Fund for the Excellent Young Teachers (No. Z2012-012).

References

1. Baelus, B.J., Peeters, F.M.: Phys. Rev. B **65**, 104515 (2002)
2. Geim, A.K., Dubonos, S.V., Palacios, J.J., Grigorieva, I.V., Henini, M., Schermer, J.J.: Phys. Rev. Lett. **85**, 1528 (2000)
3. Geurts, R., Milošević, M.V., Albino Aguiar, J., Peeters, F.M.: Phys. Rev. B **87**, 024501 (2013)
4. Du, Q.: Phys. Rev. B **46**, 9027 (1992)
5. Novoselov, K.S., Geim, A.K., Dubonos, S.V., Cornelissens, Y.G., Peeters, F.M., Maan, J.C.: Phys. Rev. B **65**, 233312 (2013)
6. Zhao, H.J., Misko, V.R., Peeters, F.M., Oboznov, V., Dubonos, S.V., Grigorieva, I.V.: Phys. Rev. B **78**, 104517 (2008)
7. Vodolazov, D.Y., Peeters, F.M., Dubonos, S.V., Geim, A.K.: Phys. Rev. B **67**, 054506 (2003)
8. Kanda, A., Baelus, B.J., Peeters, F.M., Kadowaki, K., Ootuka, Y.: Phys. Rev. Lett **93**, 257002 (2004)
9. Peng, L., Liu, Y.S., Chen, C.Z., Li, H.Y., Jia, C.L., Zou, Q.L.: J. Low Temp. Phys. **170**, 91 (2013)
10. Peng, L., Liu, Y.S., Hu, H.N., Zhang, Y.F., Xu, Y., Liu, Z.Y.: J. Supercond. Nov. Magn. **26**, 321 (2013)
11. Moshchalkov, V.V., Qiu, X.G., Bruyndoncx, V.: Phys. Rev. B **55**, 11793 (1997)
12. Schweigert, V.A., Peeters, F.M.: Physica(Amsterdam) **332C**, 266 (2000)
13. Schweigert, V.A., Peeters, F.M., Singha Deo, P.: Phys. Rev. Lett. **81**, 2873 (1998)
14. Palacios, J.J.: Phys. Rev. B **58**, 5948 (1998)
15. Baelus, B.J., Cabral, L.R.E., Peeters, F.M.: Phys. Rev. B **69**, 064506 (2004)
16. Alstrøm, T.S., Sørensen, M.P., Pedersen, N.F., Madsen, S.: Acta. Appl. Math. **115**, 63 (2011)
17. Little, W.A., Parks, R.D.: Phys. Rev. Lett. **9**, 9 (1962)
18. Chibotaru, L.F., Ceulemans, A., Bruyndoncx, V., Moshchalkov, V.V.: Nature (London) **408**, 833 (2000)
19. Bezryadin, A., Bezryadin, A., Ovchinnikov, Yu, N., Pannetier, B.: Phys. Rev. B **53**, 8553 (1996)
20. Zhao, H.W., Zha, G.Q., Zhou, S.P., Peeters, F.M.: Phys. Rev. B **78**, 064505 (2008)
21. Zhao, H.W., Zha, G.Q., Zhou, S.P.: New J. Phys. **10**, 043047 (2008)
22. Grigorieva, I.V., Escoffier, W., Richrdson, J., Vinnikov, L.Y., Dubonos, S., Oboznov, V.: Phys. Rev. Lett. **96**, 077005 (2006)
23. Gropp, W.D., Kaper, H.G., Leaf, G.K., Levine, D.M., Plumbo, M., Vinokur, V.M.: J. Comput. Phys. **123**, 254 (1996)
24. Baelus, B.J., Peeters, F.M., Schweigert, V.A.: Phys. Rev. B **63**, 144517 (2001)
25. Chaves, A., Peeters, F.M., Farias, G.A., Milošević, M.V.: Phys. Rev. B **83**, 54516 (2011)